Biosensors and Bioelectronics 74 (2015) 398–405

Contents lists available at ScienceDirect

Biosensors and Bioelectronics

journal homepage: www.elsevier.com/locate/bios

Phage–AgNPs complex as SERS probe for U937 cell identification

Germana Lentini [a], Enza Fazio [b], Federica Calabrese [a], Laura M. De Plano [a], Maria Puliafico [a], Domenico Franco [a], Marco S. Nicolò [a], Santina Carnazza [a], Sebastiano Trusso [c], Alessandro Allegra [d,*], Fortunato Neri [b], Caterina Musolino [d], Salvatore P.P. Guglielmino [a]

[a] Department of Biological and Environmental Sciences, University of Messina, Viale Ferdinando Stagno d'Alcontres 31, 98158 Messina, Italy
[b] Department of Physics and Earth Sciences, University of Messina, Viale Ferdinando Stagno d'Alcontres 31, 98158 Messina, Italy
[c] CNR-IPCF Institute for Chemical-Physical Processes, Viale Ferdinando Stagno d'Alcontres 37, 98158 Messina, Italy
[d] Department of General Surgery, Oncology and Pathological Anatomy, University of Messina, Via Consolare Valeria, 1, 98125 Messina, Italy

ARTICLE INFO

Article history:
Received 31 March 2015
Received in revised form
24 May 2015
Accepted 26 May 2015
Available online 28 June 2015

Keywords:
SERS
Phage display
U937 cells
Cell identification
Minimal residual disease

ABSTRACT

The early diagnosis of malignancy is the most critical factor for patient survival and the treatment of cancer. In particular, leukemic cells are highly heterogeneous, and there is a need to develop new rapid and accurate detection systems for early diagnosis and monitoring of minimal residual disease. This study reports the utilization of molecular networks consisting of entire bacteriophage structure, displaying specific peptides, directly assembled with silver nanoparticles as a new Surface Enhanced Raman Spectroscopy (SERS) probe for U937 cells identification *in vitro*. A 9-mer pVIII M13 phage display library is screened against U937 to identify peptides that selectively recognize these cells. Then, phage clone is assembled with silver nanoparticles and the resulting network is used to obtain a SERS signal on cell-type specific molecular targets. The proposed strategy could be a very sensitive tool for the design of biosensors for highly specific and selective identification of hematological cancer cells and for detection of minimal residual disease in a significant proportion of human blood malignancy.

1. Introduction

The discovery of new markers for the identification and discrimination of cell types, such as neoplastic cells, is one of the principal objectives in cancer diagnostics. Leukemia is one of the most blood malignancy affecting hematopoietic stem cells, bone marrow and lymphatic system. In this malignancy, the clonal population of neoplastic cells exhibits marked heterogeneity with respect to proliferation and differentiation (Bonnet and Dick, 1997; Reya et al., 2001). For this reason there is a need to develop novel approaches for the rapid and accurate detection of early-stage of leukemia and for monitoring of minimal residual disease.

Raman spectroscopy is a laser-based optical technique used for molecular analysis of a sample. A Raman spectrum obtained from cells or tissues provides a "molecular fingerprint" of a specimen, yielding detailed information about molecular bonds, conformations and intermolecular interactions. The approach is non-invasive and therefore it is ideally suited for the study of living cells. In spite of its advantages, its practical uses have been significantly limited because the Raman scattering signal is intrinsically weaker than most other fluorescence signals (Qian and Nie, 2008).

Various methods of enhancement have been developed to extend its detection limit. Among these, enhancement with noble metal nanostructures was found to be particularly interesting. Surface Enhanced Raman Spectroscopy (SERS) is a very sensitive analytic tool, suitable even for single molecule detection. In SERS, metal nanoparticles, such as silver or gold nanoparticles, can particularly enhance the Raman spectra of the molecules through amplifying the local electromagnetic field incident on a sample adsorbed on a metal surface (Aroca et al., 2005; Ko et al., 2008; Agarwal et al., 2011; Fazio et al., 2013). The sensitivity of SERS has been shown to be as high as 10^{14}–10^{15} (Nie and Emory, 1997; Kneipp et al., 1997). This technique is been regarded as a promising analytical tool for the analysis of biological samples because it provides detailed spectroscopic information, which can be translated into imaging signal and adapted to an *in vivo* imaging system (Qian et al., 2008).

Gold and silver nanoparticles could be used not only as plasmonically active substrates for label-free SERS detection, but also functionalized with different Raman reporter molecules for targeting specific ligands such as peptides, proteins, antibodies, Deoxyribonucleic acid (DNA) and antibody fragments (Zhang et al., 2011; Jokerst et al., 2011; Gao et al., 2013; Neng et al., 2013;

* Corresponding author. Fax: +39 0902212355.
E-mail address: aallegra@unime.it (A. Allegra).

http://dx.doi.org/10.1016/j.bios.2015.05.073
0956-5663/

Baniukevic et al., 2013).

More recently, novel strategies were developed using circular strand-replacement DNA polymerization with a molecular beacon as a switch and silver enhancement on magnetic nanoparticles for the specific Raman spectroscopic detection of DNA down to the sub-picomolar level (Gao et al., 2012) and combining DNAzyme assistant DNA recycling and rolling circle amplification for detection of thrombin (Gao et al., 2015).

Nuclear targeting and detection of single living eukaryotic cells was already achieved by using gold nanoparticles functionalized with a signal peptide (Xie et al., 2009). However, due to the large dimension of the nucleus and its biochemical diversity, the resulting spectra contained remarkable variations. Thus, the ability to localize SERS probes inside living cells is strictly needful to have a reproducible SERS spectrum of the cell. For this reason, it is essential to identify selective probes that can act like SERS nanotags for the recognition of target cells. Ahmad et al. (2012) performed a peptide guided SERS (pgSERS) using silver nanoparticles (AgNPs) conjugated with synthetic peptides, directed to the outer membrane of *Escherichia coli* cells.

However, peptides have disadvantages such as the folding instability, sensibility to the changes in physico-chemical parameters of the medium and high cost of synthesis and production.

Phage display is a biotechnique that allows the presentation of exogenous peptides on the surface of filamentous phage. A phage-display library consists of a pool of filamentous phage, each displaying random peptides onto one surface coat protein such as pVIII and pIII (Smith and Petrenko, 1997). The library is used to select specific phage clones that interact with particular targets, generating molecular probes with high affinity and selectivity. For this reason, phage display technology has various applications in medical, engineering and diagnostics fields (Arap, 2005; Carnazza et al., 2007, 2008; De Plano et al., 2014). Filamentous bacteriophage represent attractive alternatives to antibodies or synthetic peptides, they have some advantages such as robustness, resistance to heat, many organic solvent, acid, alkali or other stresses and a low-cost production (Petrenko and Smith, 2000; Petrenko and Vodyanoy, 2003).

In this article, a new approach for the development of biologically active AgNPs–phage networks that function as signal reporters for SERS on cell-type specific molecular targets is reported. Histiocytic lymphoma cell line (U937) is used as an *in vitro* model of cancer cells, and a 9-mer pVIII M13 phage display library is screened against U937 to identify a clone that selectively recognizes these cells. This model system represents a proof of concept study proposing a sensitive and reproducible method for cell imaging *in vitro*.

2. Materials and methods

2.1. Phage display random peptide library screening

A 9-mer random phage display library (kind gift of Prof. F. Felici) was constructed in the vector pC89, by cloning a random DNA insert between the third and fifth codon of the mature pVIII protein encoding segments of the pVIII gene (Felici et al., 1991). This library was selected towards whole U937 cells in suspension. U937 cell line was purchased from American Type Culture Collection (ATCC® CRL-1593.2™) and maintained in RPMI 1640 with L-Glutamine (Lonza, BE12-702F) supplemented with 10% fetal bovine serum (FBS, Lonza DE14-801F), penicillin (100 units/ml) and streptomycin (100 μg/ml) at 37 °C in humidified 5% CO_2 incubator. U937 cells were harvested by centrifugation at 800 rpm for 5 min, washed twice in Hank's buffered salt solution (HBSS Sigma-Aldrich pH 7.6) and resuspended at a concentration of $1 \cdot 10^6$/ml. Selection procedure was according to Cao et al. (2003) with some modifications.

Three rounds of selection were performed and recombinant phage were identified by plating them on L-agar added with X-Gal (5-bromo-4-chloro-3-indolyl-beta-D-galactopyranoside), IPTG (isopropyl thiogalactoside) and ampicillin. The presence of the insert was detected by X-gal which produces a characteristic blue dye when cleaved by β-galactosidase. Blue bacterial colonies, from third round of selection, were randomly selected. Each colony contained a single phage clone.

2.2. Elisa test

The binding capacity of the 13 phage clones to the target cells was tested in ELISA using as a negative control vector pC89.

$2.5 \cdot 10^4$ U937 cells in phosphate buffered saline solution (PBS) were dispensed in each well of a 96-well plate (Orange scientific) and incubated over night at 4 °C. They were fixed with methanol for 10 min at room temperature (RT), washed three times with Washing Buffer (PBS+0.05% Tween 20) and blocked with 100 μl of PBS+5% Lactalbumin+0.05% Tween20 for 2 h at 37 °C at 30 rpm. $1 \cdot 10^{10}$ phage clones, diluted in PBS+1% Lactalbumin+0.1% Tween-20, were added in each well and the plate was incubated for 1 h at 37 °C at 30 rpm. After three washing steps in Washing Buffer, cells were incubated with monoclonal anti-M13 peroxidase conjugate antibody (Amersham Biosciences, Buckinghamshire, UK) at a dilution of 1/5000 in PBS+1% Lactalbumin+0.1% Tween-20 (100 μl/well) for 1 h at 37 °C. After further three washing steps, antibody binding was detected by adding a 3,3′,5,5′-Tetramethylbenzidine (TMB) liquid substrate system for ELISA (Sigma-Aldrich), incubated for 45 min at room temperature and stopped with 25 μl of 1 M H_2SO_4. Optical absorbance was recorded at 450 nm (MultisKan FC ThermoScientific).

2.3. Peptide sequence analysis

The insert DNA of phage clones was amplified by Polymerase chain reaction (PCR) and sequenced. The PCR products were purified using QIAquick PCR purification kit (Qiagen) and sequenced by the DNA sequencing service of CRIBI (University of Padova, Italy) using the M13 primer-40 (5′-GTTTTCCCAGTCACGAC-3′).

The amino acid sequences were aligned according to their similarity by using the Clustal X 2.1 sequence alignment program using the IDENTITY series matrix (available at [http://clustalx.software.informer.com/2.1/]). GeneDoc (available at [http://iubio.bio.indiana.edu/soft/molbio/ibmpc/genedoc-readme.html]) was used as a tool for visualizing, editing and analyzing multiple sequence alignments of the peptides (Thompson et al., 1994; Aiyar, 2000). Statistical analysis was performed in order to calculate amino acid frequency and diversity within the pool of peptides in the selected phage clones.

2.4. Labelling of phage with FITC

$5 \cdot 10^{10}$ PFU (Plaque Forming Units) were resuspended in 200 μl Buffer Na_2CO_3/$NaHCO_3$ (pH 9.2) with 5 μl of fluorescein isothiocyanate (FITC, 5 mg/ml). Phages were incubated for 2 h in the dark on rotator at RT to allow reaction with fluorochrome. The sample was incubated at 4 °C over night with 200 μl of PEG/ NaCl and then centrifuged at 15,300*g* (Eppendorf Centrifuge 5417R) at 4 °C for 1 h. The supernatant was discarded and the pellet resuspended in 100 μl of Tris Buffered Saline [TBS, (7.88 g/L Tris–HCl, 8.77 g/L NaCl)]. Insert-less phagemid (pC89) was also labelled as negative control. Labelled phage were stored in the dark at 4 °C until utilization.

2.5. Sample preparation for fluorescence imaging

$2 \cdot 10^5$ U937 cells were put on Poly-L-Lysine (PLL) coated glass slides and fixed with cold absolute methanol for 10 min. Cells were washed three times with PBS and then incubated with 50 μl of FITC labelled-phage clone (titer $4 \cdot 10^{10}$ PFU/ml, cell/phage ratio 1:10,000) for 1 h at 37 °C. After two washings steps in PBS and one in ultrapure water, the sample was allowed to dry in air. Wild-type vector pC89 served as negative control for evaluation of background from nonspecific binding. The samples were analyzed by a fluorescence microscope (Leica DMRE) with 63 × magnification.

2.6. Preparation and characterization of Ag nanoparticles

Colloidal solutions of Ag nanoparticles were prepared by pulsed laser ablation of a high purity (99.9%) silver target immersed in distilled water, using the second harmonic (532 nm) of a neodymium-doped yttrium aluminum garnet (Nd:YAG) laser operating at 10 Hz repetition rate with a pulse width of 5 ns. The target was irradiated at the laser pulse energy of 50 mJ and for an ablation time of 15 min. The UV–vis absorption response of the Ag nanostructures was investigated, in the colloidal phase immediately after the ablation process, by means of a Perkin-Elmer Lambda 750 UV–vis spectrometer in the 190–1100 nm range. The size of the nanoparticles was determined by Dynamic Light Scattering (DLS) measurements using a Horiba NanoParticle Analyzer SZ-100 (range: 0.3 nm to 8 μm). A fraction of the same colloids was deposited on carbon substrates to carry out Scanning Electron Microscopy (SEM) characterization. SEM images were taken by a scanning electron microscope (Merlin; model ZEISS-Gemini 2) operating at an accelerating voltage of 5 kV. Energy Dispersive X-ray Analysis (EDX) was carried out using a Quantax EDX spectrometer. The EDX detected pear-shaped dimension is about 0.7 μm. X-ray photoelectron spectroscopy (XPS) spectra were acquired using a K-Alpha system of Thermo Scientific, equipped with a monochromatic Al-Kα source (1486.6 eV) and operating in constant analyzer energy (CAE) mode with a pass energy of 20 eV for high resolution spectra and a spot size of 400 μm. Transmission Electron Microscopy (TEM) images were acquired using a JEOL-JEM 2010 microscope operating at an accelerating voltage of 200 kV.

2.7. Preparation and characterization of phage–AgNPs network

The phage–AgNPs network was prepared by incubating AgNPs with the phage clones, resuspended in TBS buffer, in a 4:1 ratio at 30 °C in orbital shaking at 320 rpm (KS130 Basic IKA) over night.

In order to separate the AgNPs–phage network from the unbounded phage and free silver, networks were purified by centrifugation at 20,800*g* for 30 min. The complex was stored at 4 °C until utilization.

2.8. Sample preparation for Raman analysis

2.8.1. U937 cells

$2 \cdot 10^5$ cells were put on PLL coated CaF_2 slides and fixed with cold absolute methanol for 10 min. After two washings steps in PBS and one in ultrapure water, the sample was allowed to dry in air.

2.8.2. Phage

50 μl of phage suspension were put on PLL coated CaF_2 slides. The sample was allowed to dry in air.

2.8.3. U937 + phage

$2 \cdot 10^5$ U937 cells were put on PLL coated CaF_2 slides and fixed with cold absolute methanol for 10 min. After three washing steps with PBS, cells were incubated with 50 μl of phage clone (titer $4 \cdot 10^{10}$ PFU/ml, ratio cell/phage 1:10,000) for 1 h at 37 °C. After washing two times in PBS and one in ultrapure water, the sample was allowed to dry in air.

2.8.4. AgNPs + U937

$2 \cdot 10^5$ cells were put on PLL coated CaF_2 slides and fixed with cold absolute methanol for 10 min. After three washing steps with PBS, cells were incubated with 50 μl of AgNPs for 1 h at 37 °C. After washing two times in PBS and one in ultrapure water, the sample was allowed to dry in air.

2.8.5. AgNPs–phage

50 μl of AgNPs–phage network suspension were put on PLL coated CaF_2 slides. The sample was allowed to dry in air.

2.8.6. U937 + AgNPs–phage

$2 \cdot 10^5$ U937 cells were put on PLL coated CaF_2 slides and fixed with cold absolute methanol for 10 min. After three washing steps with PBS, cells were incubated with 50 μl of Ag–phage network for 1 h at 37 °C. After washing two times in PBS and one in ultrapure water, the sample was allowed to dry in air before characterization with Raman microscopy in the 200–1800 cm^{-1} range.

The samples were analyzed by the micro-Raman spectroscopy using an Horiba XploRa spectrometer equipped with an Olympus BX40 microscope, a Peltier cooled charge coupled device (CCD) sensor and a 532 nm (2.33 eV) laser as the excitation source. An acquisition time of 100 s allowed a sufficient signal/noise (*S*/*N*) ratio. Measurement parameters did not induce cell damages.

To ensure reproducibility, experiments were performed in triplicate.

3. Results and discussion

3.1. Phage display random peptide library screening and sequence analysis

We screened a 9-mer pVIII M13 phage display peptide library toward whole diffuse histiocytic lymphoma (U937) cells in suspension. The most reactive phage clones showing a specific U937 cells-binding, from third round of affinity selection, were amplified and their DNA was sequenced to determine the amino acid sequences of the displayed peptides. The deduced amino acid sequences were aligned by using CLUSTALX 2.1 software based on IDENTITY matrix, and the consensus sequence was obtained by using GENEDOC software. All sequences contained two positively charged amino acid residues (lysine and arginine) in the amino terminal region and non-polar amino acid residues in the central positions. These regions may be directly involved in the cell–target interaction. Among all peptides, EIII1 phage sequence showed the most significant similarity with consensus when all the clone sequences were re-aligned with this (Fig. 1).

The relative binding of the phage clones was estimated by ELISA test, using as negative control the insert-less vector pC89. The results showed that all selected phage clones had a similar reactivity and specificity for U937 cells (data not shown). Because of sequence similarities and ELISA results among affinity-selected clones, phage clone displaying the deduced sequence RKIVHAQTP, named EIII1 was chosen as prototype to test the self-assembly with silver nanoparticles.

3.2. Fluorescence Image Analysis

In order to confirm the recognition of the target cells, we

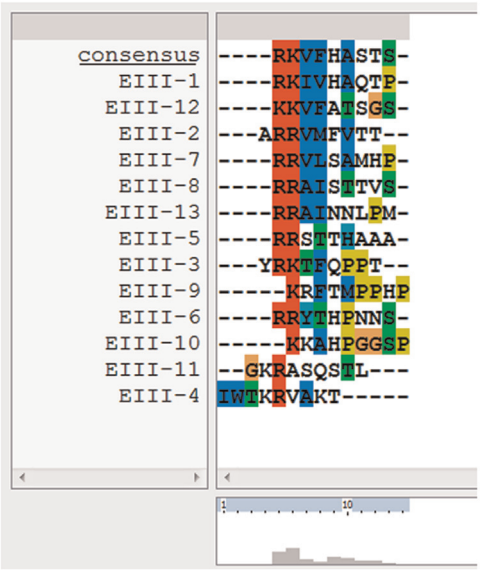

Fig. 1. Alignment of phage-displayed peptides. The deduced amino acid sequences were aligned by using CLUSTALX 2.1 with the consensus sequence obtained by GENEDOC. Dashes indicate gaps used to maximize the alignment. This alignment shows conserved positively charged amino acid residues in the N-terminal region (K and R), flanked by nonpolar amino acids such as Valine (V), Isoleucine (I), Leucine (L) and Alanine (A).

directly labelled EIII1 with FITC amine-reactive fluorochrome for *in vitro* imaging. Even though this fluorochrome labels the phage pVIII major coat protein, as demonstrated by Jaye et al. (2004) the binding selectivity of peptides displayed on capsid protein was maintained. EIII1 was found to specifically bind to U937, as seen by the bright green fluorescence of FITC (Fig. 2a and b). Fluorescence was quenched when using pC89 insert-less phagemid indicating a specificity of the peptide expressed by EIII1 (Fig. 2c).

3.3. Ag nanoparticles

UV–vis optical absorption spectra of Ag nanocolloids showed a well-defined absorption band (Fig. 3a). The maximum of this absorption band, due to a surface plasmon resonance, was centered at 406 nm. The broadening of the plasmon peak clearly indicated the presence of differently sized nanoparticles (NPs). Their size and distribution were determined by DLS and TEM measurements (Fig. 3b). The Ag samples consisted of a distribution of nearly spherical nanoparticles, whose size is smaller than 10 nm with a PDI value of 0.4 (where 0.4 refers to the most polydisperse population); some nanoparticles larger than 50 nm were also observed. The AgNPs were characterized by a *Z* potential value of −27 mV, indicating a high stability of the colloidal solution, and ruling out the possibility of aggregation processes.

3.4. AgNPs–phage network

Incubation of EIII1 with AgNPs resulted in the formation of a yellowish colored solution after overnight incubation at 30 °C. It was firstly characterized by UV–vis optical absorption spectroscopy. The spectrum of AgNPs–EIII1 solution exhibited a well-defined intense band centered at 406 nm, ascribed to the AgNPs Surface Plasmon Resonance contribution and a less intense one at around 269 nm, related to aromatic residues of phage (Fig. 3c). This contribution was similar to that observed in literature (Schmid, 2001; Overman et al., 2005).

Subsequently the AgNPs–EIII1 complexes were characterized by SEM. Some networks, consisting of entire bacteriophage structure directly assembled with AgNPs, were evident from SEM image, as shown in Fig. 3d. Particularly closed-packed Ag–phage nanostructures were formed on the assembled phage films on all the micrometer-length scale investigated (Fig. 3e). Fig. 3f shows the Ag 2p XPS spectra of Ag-NPs–EIII1 network. The Ag 3d lineshape shows two strong peaks at 374.1 and 368.1 eV, due to $Ag3d_{3/2}$ and $Ag3d_{5/2}$, respectively. Further, the XPS detection of C, O, Cl and mainly of N and Ag is a benchmark suggesting phage adsorption near AgNPs. This result suggests that phage has high affinity for Ag, index of the assembly of Ag NPs with the phage. The XPS compositional data are confirmed by EDX results, as shown in Table 1.

Most of the AgNPs are in the regions in which the EDX probe shows the presence of nitrogen, carbon and oxygen species. This result again indicates that the phage structures are decorated and/or chemically linked to the AgNPs.

The surface of the filamentous phage contains more than 2700 copies of its major coat protein, pVIII, and about 50% of these proteins display cell-binding peptides (Wang et al., 2006). Thus, the successful grafting of the EIII1 with the AgNPs occurred probably by the N-terminal part of pVIII proteins. This was consistent with a specific interaction between particular functional groups of the pVIII coat protein and the AgNPs surface. The zeta potential of the EIII1 and AgNPs–EIII1 network, calculated from the electrophoretic mobility, was −25 mV and −15 mV, respectively. The zeta potential value of the AgNPs–EIII1 network is explained on the basis of the distribution of the phage respect to AgNPs and their electrostatic interactions. Further, these results indicate that the AgNPs–EIII1 assemblies are fairly stable.

3.5. Raman analysis

The interaction between AgNPs–EIII1 network and U937 cells

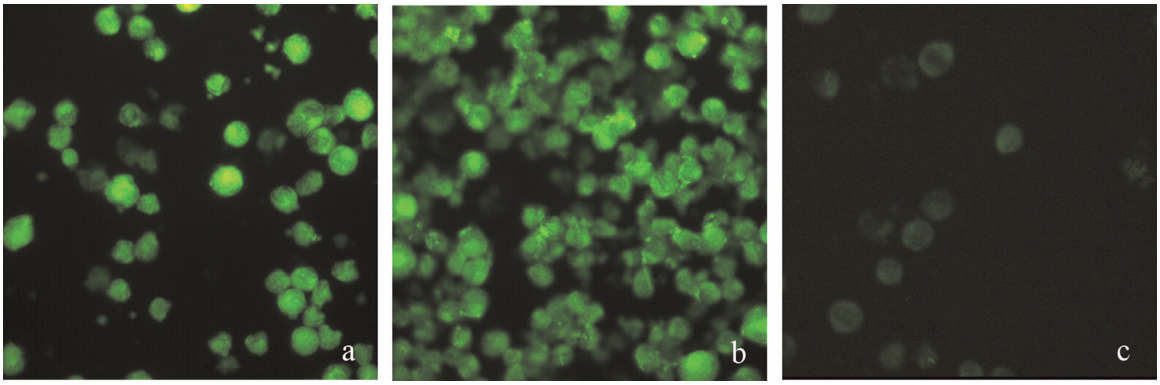

Fig. 2. Validation of phage clones by fluorescence microscopy. U937 cells were incubated with FITC-labelled phage: EIII1 (a, b) and insert-less vector pC89 (c).

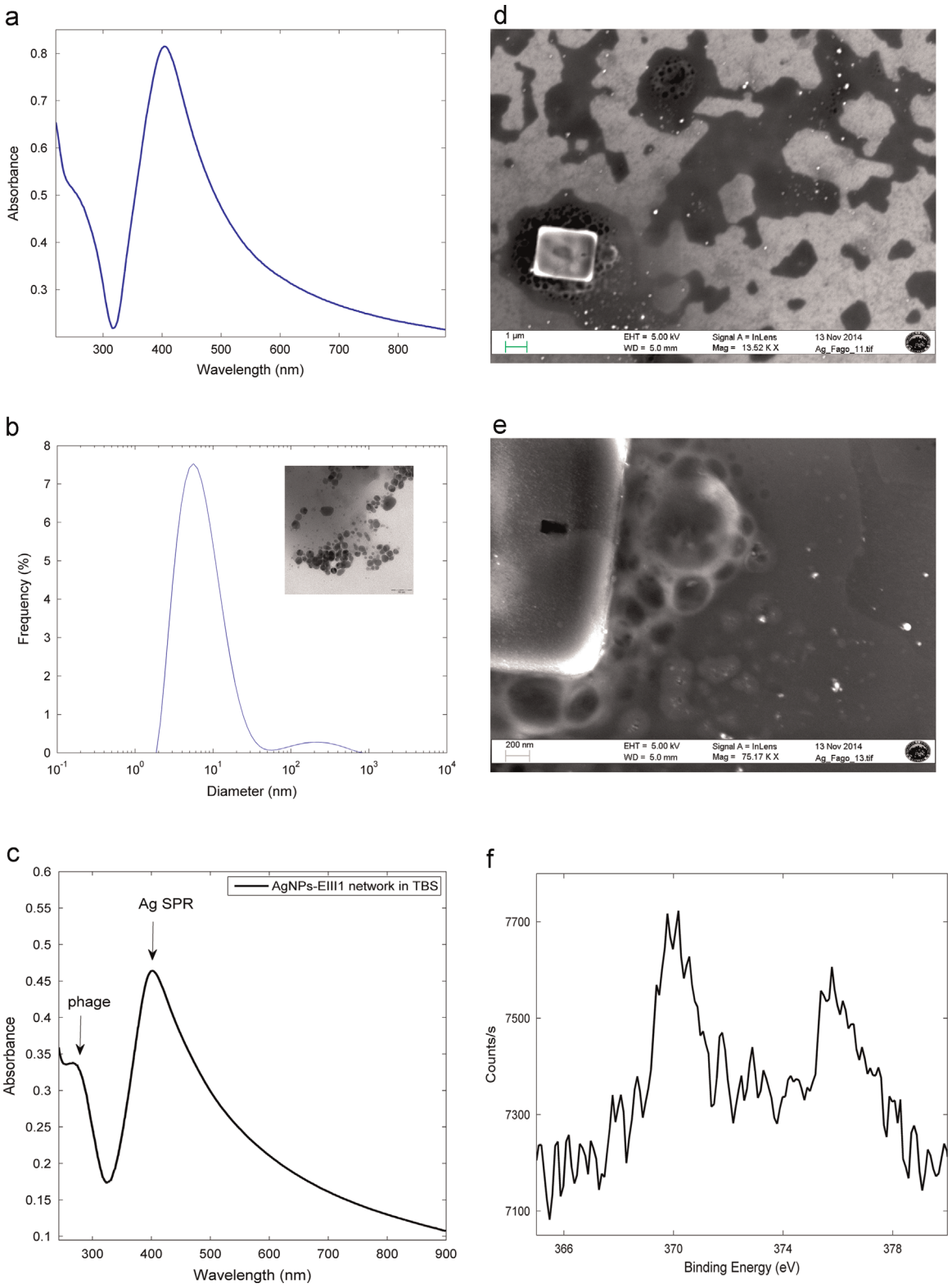

Fig. 3. UV–vis optical absorbance (a), DLS and TEM (b) data of silver nanoparticles. UV–vis optical absorbance (c), SEM images (d,e) and XPS analysis (f) of AgNPs–EIII1 network.

was further evaluated by Raman spectroscopy.

Firstly, we analyzed the Raman spectra of U937 and EIII1 alone (Fig. 4). Raman spectra recorded on different samples as well as on different positions within the samples, were similar. The Raman spectrum (Fig. 4) of U937 cells shows many peaks assignable to proteins (901.5, 990.4, 1269 and 1675 cm^{-1}), nucleic acids (1094 and 1345 cm^{-1}) and saccharides (1462 cm^{-1}) (Allegra et al., 2014). The presence and mainly the position of the Raman peaks, generally observed in U937 cells, are strongly influenced by cell fixation methods (Chan et al., 2009; Ranc et al., 2013). In our case, the treatment with methanol induced the intensity increase of the contributions assignable to membrane proteins and

Table 1
EDX and XPS elemental composition of AgNPs–EIII1 network.

Element	Series	EDX C norm (wt%)	EDX C atom (wt%)	XPS C atom (%)
Ag	L	88.0	49.5	2.20
C	K	5.2	26.3	65.0
O	K	4.4	16.7	27.0
N	K	1.3	5.8	3.90
Cl	K	1.1	1.7	1.90

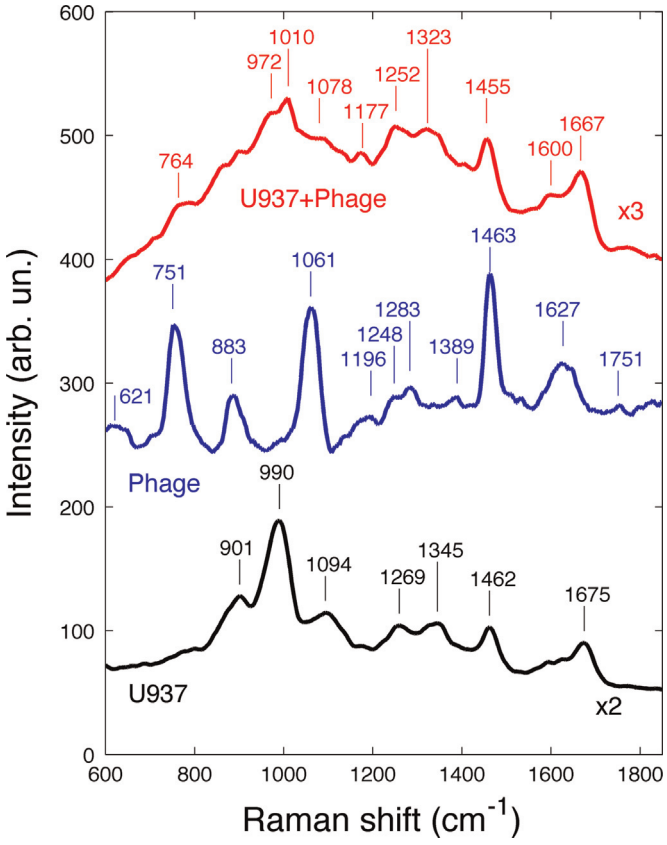

Fig. 4. Raman spectra of U937 cells, EIII1 phage and U937–EIII1 complex.

carbohydrates. This behavior is explained on the basis of the action of methanol on membrane lipids. On the other hand, the peaks ascribed to the protein composition remained almost unchanged. Despite this, the U937 methanol treatment did not modify the ability of the phage clone to recognize its cellular target, as shown below by fluorescence analysis.

The Raman spectrum of EIII1 (see Fig. 4) was characterized by some contributions located at 1196, 1248, 1283, 1388, 1627 and 1751 cm^{-1}, attributed to the stretching mode of amide, and other peaks centered at 621, 751.7 and 1463 cm^{-1}, due to the aromatic residues of phage coat proteins (Aslanian et al., 1982; Aubrey and Thomas, 1991). Moreover, the Raman spectrum of EIII1 showed a weak band at 883.5 cm^{-1} and an intense contribution at 1062 cm^{-1}, referred to the PO^{2-} stretching mode of packaged ssDNA phage (Benevides et al., 1991).

Raman measurements were then carried out on U937–EIII1 assemblies in order to evaluate the structural modifications of U937 after the cellular target recognition by phage. In Fig. 4 is shown the Raman spectrum of U937–EIII1 complex. It is evident that the U937 Raman features due to proteins, nucleic acids and saccharides contributions shifted to lower wavenumber (1078, 1252, 1323, 1455 and 1667 cm^{-1}). A further indication of the interaction of the whole phage structure with the U937 cells was highlighted by the appearance of new Raman peaks, centered at 764, 972, 1010, 1177 and 1600 cm^{-1}. The shift in Raman peaks is related to the interaction of engineered phage peptides with the U937 cells (Miskovsky et al., 1998; Fabriciova et al., 2004; Jurasekova et al., 2009). The new peaks are ascribed to stretching modes of saccharides and proteins, suggesting that phage-binding target is represented by a cellular glycoprotein (Lu et al., 2013).

The major biochemical constituents in U937–EIII1 complex are proteins, nucleic acids and saccharides. Although the specific recognition allows discriminating the superimposition of many different chemical entities, derived from phage and cell, it is not easy to analyze as many bands occur at the same positions and overlap. Marker bands, which are specific to a certain type of molecule, were assigned to some of the components. It was not possible to use the strongest band in the spectrum of a specific compound as a marker, since it could overlap with bands from other molecules and not all the constituents could be identified through their Raman spectra as some of the bands are hidden.

For this reason, SERS was used to evaluate specific U937 structural changes since preferential enhancement takes place in dependence on the way the phage pVIII protein binds to the AgNPs surface, and then interacts with the U937 cells. In Fig. 5 are shown the Raman spectra of AgNPs–U937 and AgNPs–EIII1 assemblies. The Ag–U937 spectrum was similar to the U937 one while the AgNPs–EIII1 network showed some differences respect to the EIII1 phage. The main differences were: i) a significant shift of the Raman features associated to the protein contributions observed at 1173, 1275, 1369, 1739 and 1838 cm^{-1} and ii) the enhancement of the Raman peaks associated both to proteins and DNA contributions (this latter are observed at 880.9 and 1059 cm^{-1}); iii) the slight enhancement and the shifting from 621, 751.7, 1463 and 1627 cm^{-1} to 644.5, 754.3, 1461 and 1620 cm^{-1} of the EIII1. As shown by literature, these spectral changes depend on the

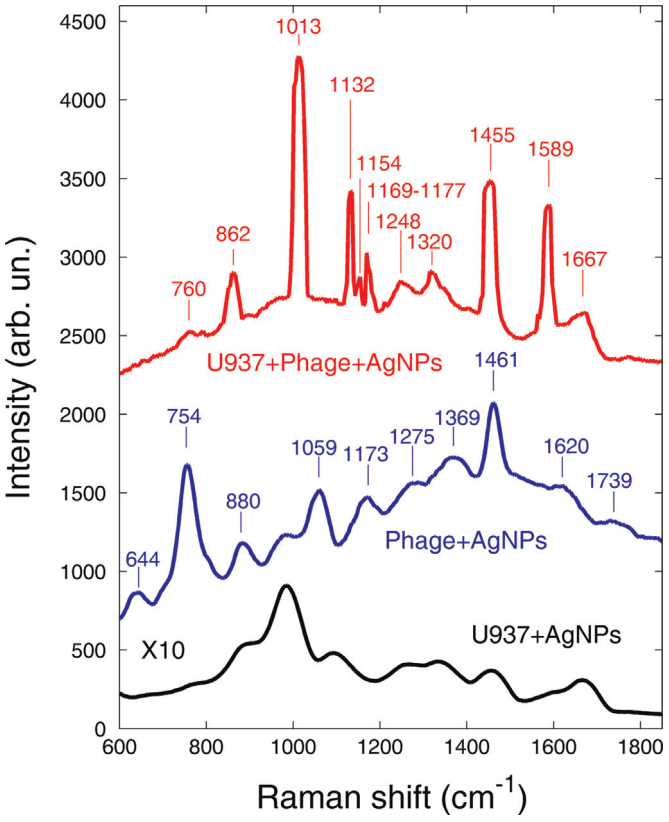

Fig. 5. Raman spectra of Ag–U937 cells, AgNPs–EIII1 and AgNPs–EIII1+U937 complex.

orientation and the distance of the molecules from the surface of the metal nanostructures (Podstawka et al., 2004). However, this behavior is indicative of the stretching modes deformation of exposed residues on the major capsid proteins, suggesting their direct interaction with AgNPs in the network assembly (Stewart and Fredericks, 1999). If the Raman vibrations of the reporter molecules are narrow and do not overlap, the inclusion of AgNPS–EIII1 network into U937 cells (whose characteristic vibrational signals act as Raman reporter) can potentially monitor simultaneously different and new interaction. In this contest, we carried out Raman measurements on the U937–EIII1–AgNPs system which spectrum is shown in Fig. 5.

U937 cells targeted by EIII1–AgNPs network showed the appearance of new Raman scattering peaks at 862.6, 1132 and 1154 cm^{-1} in addition to the enhancement intensity of some of the fundamental U937 Raman features (specifically, the contributions related to proteins centered at 760.6, 1013, 1154, 1169, 1177,1248, 1320, 1455, 1589 and 1667 cm^{-1}). These spectral features refer to the oligosaccharides complexes, namely molecules involved in probe–target interaction (ur Rehman et al., 2012). The strong electric field near the AgNPs allowed a different coupling mechanism between the optical electric field and the vibration. The selection rule for this process differed markedly from the usual Raman selection rules. The SERS-induced occurrence of new Raman peaks was attributed to the lowering of the symmetry of the investigated molecules or to the presence of a steep field close to the nanoparticles metal surface (Fazio et al., 2012).

In this case, EIII1–AgNPs complexes "bind" a cell-specific target probably represented by a glycoprotein receptor localized on the plasma membrane. Hence, we prepared AgNPs–phage networks that, in addition to targeting cells, could function as signal reporters for SERS spectroscopy. A similar approach was adopted by Souza et al. (2006) that achieved specific biomolecule targeting using engineered filamentous bacteriophage fd displaying the targeting peptide RGD-4C on the surface of its pIII protein. These filamentous viruses were assembled with gold nanoparticles in biologically active molecular networks and used to label cells in suspension. The spontaneous organization of these networks was further manipulated by incorporation of imidazole, a metal-binding molecule. However, these networks showed a high background SERS signal that lowered the assay signal-to-noise ratio, exposing the tags to spectral changes and aggregation. Similarly to Souza et al., our proposed network has the advantage to integrate the unique signal reporting properties of AgNPs while preserving the biological properties of phage without the use of additional SERS signal reporters (*e.g.* imidazole or bis-bipyridyl complexes of ruthenium). Moreover, no preliminary informations about the nature of target are needed. Overall, it emerges that the molecular networks consisting of entire bacteriophage structure directly assembled with AgNPs represent a new SERS probe for U937 cells identification *in vitro*, potentially extensible for the detection of other cell-type specific molecular targets. Particularly, the proposed strategy could be a very sensitive tool for the identification of hematological cancer cells and the detection of minimal residual disease in a significant proportion of human blood malignancy.

Ultimately, the proposed approach could represent a method for the rapid identification of neoplastic cells and, at the same time, AgNPs–phage network could be used as carrier for therapeutic drugs and for cancer cells targeting and killing. In fact, it is well known that AgNPs are selectively involved in the disruption of mitochondrial respiratory chain, leading to ROS production and to the interruption of ATP synthesis which cause DNA damage (Rosarin et al., 2012).

4. Conclusions

Raman spectroscopy is a rapid and non-destructive technique, sensitive to chemical and physical changes of biological molecules. It can be used to recognize, with high sensitivity, the changes that take place in nucleic acid, proteins, lipids and carbohydrate quantities and/or conformation. In spite of its advantages, the Raman scattering signal is intrinsically weak, so various methods of enhancement have been developed to extend its detection limit. SERS is a variation of Raman spectroscopy which offers significant enhancement of the signal in the presence of metal nanoparticles, making detection faster, simpler, and more accurate. However, the main challenge with SERS is the attainment of repeatable and reproducible spectra. The SERS approach developed in this research represents an important method for reducing the complexity of SERS analysis of eukaryotic cells, allowing to identify cell-type-specific molecular targets. The human promonocytic cell line U937 is used as an *in vitro* model of cancer cells, and a 9-mer pVIII M13 phage display library is screened against U937 to identify a clone that selectively recognizes these cells. The Ag nanostructured-bacteriophage network represents a new SERS probe for U937 cells identification, potentially extensible for the detection of other neoplastic cells and, in turn, for the detection of minimal residual disease. This model system represents a proof of concept study for the design of highly sensitive and selective biosensors for rapid and non-invasive cancer-cell detection.

Acknowledgments

This work was partially funded by Italian Ministry of Education, University and Research (MIUR) by means of the national Program PON R&C 2007–2013, project "*Hyppocrates–Sviluppo di Micro e Nano-Tecnologie e Sistemi Avanzati per la Salute dell'uomo* (PON02 00355)". Authors also gratefully acknowledge financial support of A.B.A.L. onlus Messina (Italy) (http://abalmessina.it/) for clone selection and the use of the XploRA Raman spectrometer, and the kind gift of phage-display libraries from Prof. Franco Felici.

References

Agarwal, N., Fazio, E., Neri, F., Trusso, S., Castiglioni, C., Lucotti, A., Santo, N., Ossi, P. M., 2011. Cryst. Res. Technol. 46, 836–840.
Ahmad, I., Athamneh, M., Senger, R.S., 2012. Appl. Environ. Microbiol. 78 (21), 7805–7808.
Aiyar, A., 2000. Methods Mol. Biol. 132, 221–241.
Allegra, A., Fazio, E., Franco, D., Nicolò, M., Trusso, S., Neri, F., Musolino, C., Guglielmino, S., 2014. Leuk. Lymphoma 3, 1–3.
Arap, M.A., 2005. Genet. Mol. Biol. 28 (1), 1–9.
Aroca, R.F., Alvarez-Puebla, R.A., Pieczonka, N., Sanchez-Cortes, S., Garcia-Ramos, J. V., 2005. Adv. Colloid Interface Sci. 116 (1–3), 45–61.
Aslanian, D., Rontò, G., Toth, K., 1982. Acta Phys. Acad. Sci. Hung. 53 (1–2), 25–32.
Aubrey, K.L., Thomas Jr., G.J., 1991. Biophys. J. 60, 1337–1349.
Baniukevic, J., Boyaci, I.H., Bozkurt, A.G., Tamer, U., Ramanavicius, A., Ramanaviciene, A., 2013. Biosens. Bioelectron. 43, 281–288.
Benevides, J.M., Stow, P.L., Ilag, L.L., Incardona, N.L., Thomas Jr., G.J., 1991. Biochemistry 30 (20), 4855–4863.
Bonnet, D., Dick, J.E., 1997. Nat. Med. 3, 730–737.
Cao, J., Zhao, P., Miao, X.H., Zhao, L.J., Xue, L.J., Qi, Z.T., 2003. Cell Res. 13 (6), 473–479.
Carnazza, S., Gioffrè, G., Felici, F., Guglielmino, S., 2007. J. Phys.: Condens. Matter 19 (395011), 13.
Carnazza, S., Foti, C., Gioffrè, G., Felici, F., Guglielmino, S.P.P., 2008. Biosens. Bioelectron. 23 (7), 1137–1144.
Chan, J.W., Taylor, D.S., Thompson, D.L., 2009. Biopolymers 91 (2), 132–139.
De Plano, L.M., Calabrese, F., Lentini, G., Nicolò, M.S., Franco, D., Fazio, E., Trusso, S., Allegra, A., Neri, F., Guglielmino, S.P.P., 2014. New Biotechnol. 31, S107.
Fabriciova, G., Sanchez-cortes, S., Garcia-Ramos, J.V., Miskovsky, P., 2004. Biopolymers 74, 125–130.
Fazio, E., Neri, F., Savasta, S., Spadaro, S., Trusso, S., 2012. Phys. Rev. B 85 (195423), 7.
Fazio, E., Neri, F., Valenti, A., Ossi, P.M., Trusso, S., Ponterio, R.C., 2013. Appl. Surf. Sci. 278, 259–264.

Felici, F., Castagnoli, L., Musacchio, A., Jappelli, R., Cesareni, G., 1991. J. Mol. Biol. 222, 301–310.
Gao, F., Lei, J., Ju, H., 2013. Anal. Chem. 85, 11788–11793.
Gao, F., Zhu, Z., Lei, J., Ju, H., 2012. Chem. Commun. 48, 10603–10605.
Gao, F., Du, L., Tang, D., Lu, Y., Zhang, Y., Zhang, L., 2015. Biosens. Bioelectron. 66, 423–430.
Jaye, D.L., Geigerman, C.M., Fuller, R.E., Akyildiz, A., Parkos, A., 2004. J. Immunol. Methods 295, 119–127.
Jokerst, J.V., Miao, Z., Zavaleta, C., Cheng, Z., Gambhir, S.S., 2011. Small 7 (5), 625–633.
Jurasekova, Z., Marconi, G., Sanchez-cortes, S., Torreggiani, A., 2009. Biopolymers 91, 917–927.
Kneipp, K., Wang, Y., Kneipp, H., Perelman, L.T., Itzkan, I., Dasari, R.R., Feld, M.S., 1997. Phys. Rev. Lett. 78, 1667–1670.
Ko, H., Singamaneni, S., Tsukruk, V.V., 2008. Small 4 (10), 1576–1599.
Lu, X., Liu, Q., Benavides-Montano, J.A., Nicola, A.V., Aston, D.E., Rasco, B.A., Aguilar, C., 2013. J. Virol. 87 (6), 3130–3133.
Miskovsky, P., Jancura, D., Sanchez-Cortes, S., Kocisova, E., Chinsky, L., 1998. J. Am. Chem. Soc. 120, 6374–6379.
Neng, J., Harpster, M.H., Wilson, W.C., Johnson, P.A., 2013. Biosens. Bioelectron. 41, 316–321.
Nie, S.M., Emory, S.R., 1997. Science 275, 1102–1106.
Overman, S.A., Bondr, P., Maiti, N.C., Thomas Jr., G.J., 2005. Biochemistry 44, 3091–3100.
Petrenko, V.A., Smith, G.P., 2000. Protein Eng. 13 (8), 101–104.
Petrenko, V.A., Vodyanoy, V.J., 2003. J. Microbiol. Methods 53 (2), 243–252.
Podstawka, E., Ozaki, Y., Proniewicz, L.M., 2004. Appl. Spectrosc. 58, 570–580.
Qian, X., Peng, X.H., Ansari, D.O., Yin-Goen, Q., Chen, G.Z., Shin, D.M., Yang, L., Young, A.N., Wang, M.D., Nie, S., 2008. Nat. Biotechnol. 26, 83–90.
Qian, X.M., Nie, S.M., 2008. Chem. Soc. Rev. 37, 912–920.
Ranc, V., Srovnal, J., Kvítek, L., Hajduch, M., 2013. Analyst 138 (20), 5983–5988.
Reya, T., Morrison, S.J., Clarke, M.F., Weissman, I.L., 2001. Nature 415 (6859), 105–111.
Rosarin, F.S., Arulmozhi, V., Nagarajan, S., Mirunalini, S., 2012. Asian Pac. J. Trop. Med. 6 (1), 1–10.
Schmid, F.X., 2001. Encyclopedia Life Sci, Introductory articles, Bridgewater R, 1–4.
Smith, G.P., Petrenko, V.A., 1997. Chem. Rev. 97 (2), 391–410.
Souza, G.R., Christianson, D.R., Staquicini, F.I., Ozawa, M.G., Snyder, E.Y., Sidman, R.L., Miller, J.H., Arap, W., Pasqualini, R., 2006. Proc. Natl. Acad. Sci. USA 103 (5), 1215–1220.
Stewart, S., Fredericks, P.M., 1999. Spectrochim. Acta Part A 55, 1641–1660.
Thompson, J.D., Higgins, D.G., Gibson, T.J., 1994. Nucleic Acids Res. 22 (22), 4673–4680.
ur Rehman, I., Movasaghi, Z., Rehman, S., 2012. Series in Medical Physics and Biomedical Engineering. CRC Press, Taylor & Francis Group, Boca Ranton, FL.
Wang, Y.A., Yu, X., Overman, S., Tsuboi, M., Thomas Jr., G.J., Egelman, E.H., 2006. J. Mol. Biol. 361 (2), 209–215.
Xie, W., Wang, L., Zhang, Y., Su, L., Shen, A., Tan, J., Hu, J., 2009. Bioconjugate Chem. 20 (4), 768–773.
Zhang, Y., Hong, H., Myklejord, D.V., Cai, W., 2011. Small 7, 3261–3269.